– ORIGINAL RESEARCH –

 # or Words:

Propagation Mapping:

A Precision Framework for Reconstructing the Neural Circuitry of Brain Maps

Jules R. Dugré, PhD [1];

[1] Department of Psychology, College of Literature, Science, and the Arts, University of Michigan, USA.

Corresponding authors
Jules Roger Dugré, PhD
Department of Psychology,
College of Literature, Science, and the Arts,
University of Michigan, Ann Arbor, MI, USA 48109
Email: jdugre@umich.edu

Abstract

Human brain mapping has traditionally relied on univariate approaches to characterize regional activity, an assumption that is increasingly being challenged. While functional connectivity offers a promising alternative, it fails to capture signal amplitude, which is essential for a comprehensive understanding of the brain's biological organization. The current study introduced and validated propagation mapping, a novel framework designed to reconstruct the neural circuitry underlying human brain maps. By modeling the interdependence of regional signal amplitude and connectivity, the spatial organization of brain maps could be predicted with near-perfect accuracy. This precision remained stable across task contrasts, parcellation atlases, and both short- and long-range connections. Critically, propagation mapping preserved each individual's functional fingerprint, enabling reliable study of inter-individual differences in brain–behavior relationships. As a biologically informed and accessible representation of brain organization, propagation mapping provides a powerful alternative to traditional regional analyses and opens new avenues for discovery in neurological and psychiatric neuroimaging research.

Keywords: - Activity - Connectivity – Brain Mapping - Methodology

Main

From the earliest days of human brain mapping, researchers have relied on statistical parametric maps to infer brain structure and function. With the advent of MRI, voxelwise maps became central to neuroimaging, spanning modalities from metabolism and morphometry to BOLD signal amplitude [1-3]. Mass-univariate analyses were initially justified by the assumption that hemodynamic responses vary across regions even under identical neuronal activation [4]. Yet despite decades of methodological advances, replicability remains a persistent challenge— as shown by poor test–retest reliability in common tasks [5]. These issues likely stem from both methodological variability [6-8] and deeper conceptual limitations. These include the traditional assumption that brain regions work as isolated units [9,10]. Connectivity-based approaches offer a promising alternative. However, they also suffer from limited reliability [11]. While increasing scan length can improve reliability of connection-level estimates [12], regional measures (e.g., ALFF, ReHo) tend to yield greater intraclass correlations [13-15], which may be attributable to their oversimplification of biological functioning. Balancing measurement reliability with neurobiological precision remains a central challenge, underscoring the need for approaches that integrate both regional and connectivity perspectives.

Conceptualizing the brain as a network of interconnected nodes is essential, yet a critical piece of the puzzle remains missing. Correlation between fMRI time series quantifies the similarity of waveform shapes, as a measure of temporal synchrony but ignores relative amplitude. However, evidence suggests that regional BOLD activation and functional connectivity are complementary rather than mutually exclusive. Since the early days of MRI [16], statistical maps of BOLD amplitude have been shown to closely align with regional connectivity

strength [17-20]. This relationship suggests that brain regions with stronger functional connectivity (FC) to the rest of the brain have greater metabolic demand (e.g., oxygen, glucose) [21,22], resulting in greater blood flow fluctuations, as reflected in BOLD signal amplitude. Strikingly, recent work has shown that regional brain activity can be predicted by a weighted sum function of an individual's resting-state FC matrix [23,24]. Indeed, researchers achieved moderate-to-high prediction accuracy at a subject-level ($r \approx 0.70$) using this approach [23] highlighting the importance of considering both regional activity and connectivity for a comprehensive understanding of the biological functioning of the brain. While these findings underscore the tight coupling between regional activity and connectivity, it also suggest that task-evoked activity may operate on a general and stable underlying functional architecture [25-27].

The Current Study

The goal of this paper is to introduce and validate a novel framework, propagation mapping, designed to predict the spatial patterns of brain maps by reconstructing their underlying neural circuitry. The core assumption behind propagation mapping is that if brain maps can be accurately predicted using a weighted sum, then the weighted connectome prior to summation must accurately capture the connectivity patterns of the brain map. This reconstructed connectome, referred to as a *propagation map*, is therefore a biologically informed representation of signal propagation that can be used to generate new hypotheses through graph metrics and connectome-based predictive modeling [28]. Although spatial patterns of brain maps vary widely across individuals and conditions, the underlying functional architecture is thought to remain largely stable, serving as a blueprint for brain organization. Therefore, relying on group-level FC estimates from a large sample is assumed to provide a robust framework for estimating subject-level circuitry. Therefore, I hypothesized that integrating such data would

enhance the prediction of subject-specific brain maps, relative to what others have found using subject's own FC matrix [23]. I further hypothesized that incorporating structural covariance (SC) estimates would yield better prediction of subject-specific brain maps. Indeed, prior work has shown that morphometric variations systematically covary between regions and mirror FC [29,30], indicating that anatomical properties such as volume may constrain and guide functional interactions. The current manuscript is divided in two complementary studies to validate the method:

In Study 1, the aim was to identify the optimal biological model of propagation mapping for task-evoked BOLD activity maps and to test the stability of its predictive accuracy across task contrasts, parcellation atlases, and short- and long-range connections. As suggested above, it was hypothesized that the predictive accuracy of subjects' task-evoked activity maps could be improved by incorporating stable FC and SC estimates. I further hypothesized that the prediction accuracy would be stable across task contrasts, parcellation atlases, and distance of connectivity.

In Study 2, the goal was to investigate the prediction accuracy of propagation mapping at the group level using resting-state low-frequency oscillation maps from an independent sample. While subject-level prediction may benefit from using group-level connectivity estimates, it can also obscure individual brain activity patterns. To account for this possibility, it was tested whether propagation mapping preserves the uniqueness of brain activity, known as functional fingerprint [31,32]. It was hypothesized that propagation mapping would preserve both group-level information and individual-specific patterns of brain activity, serving as a versatile tool to reconstruct neural circuits from the spatial organization of brain maps.

Results: Study 1

Biological Models

Propagation mapping approach is displayed in Fig 1A. Different biological models were tested to identify how well propagation mapping perform in terms of predictive accuracy. Across six different task conditions, the best fitting biological model was the combination of positive edges of FC and SC matrices with equal weighting (*mean rs* ranging from .938 – 0.971), followed by unique contribution of positive edges of SC matrix (*mean rs* ranging from 0.926 – 0.962). The least performing model was the use of full FC matrix (*mean rs* ranging from 0.663 – 0.749) (see Supplementary Table 1. for statistical differences between models across task conditions).

Task Contrasts & Parcellations

Propagation mapping using positive edges of the FC and SC matrices with equal weighting show high predictive accuracy across all task contrasts (Fig 1B). More precisely, Wilcoxon signed-rank tests revealed that Checkerboard (*mean r* = .971, standard deviation [SD] = 0.012), Sentence Reading (*mean r* = .967, SD = 0.018), and Sentence Listening (*mean r* = .967, SD = 0.019) did not differ from each other ($q > 0.05$). Both Button Press conditions (Right: *mean r* = .940, SD = 0.030; Left: *mean r* = .938, SD = 0.033) did not differ from each other ($q > 0.05$) and show significantly lower predictive accuracy than the other task contrasts (Sentence reading = Checkerboard = Sentence listening > Calculation > Left Button Press = Right Button Press) (Supplementary Table 2).

Across the different task contrasts, Schaefer's parcellation performed systematically higher than all the other parcellation schemes ($q < 0.05$), except in the two Button Press

conditions. In the Left Button Press condition, Gordon parcellation showed slightly higher predictive performance than Schaefer's parcellation ($q < 0.05$). In the Right Button Press, no significant difference was found between Schaefer's parcellation and Glasser's parcellation ($p = 0.682$), suggesting that both had the highest predictive performance for that condition (Supplementary Table 3).

Short-range vs. Long-range Connections

Despite some significant differences between short-range and long-range connections, propagation mapping does not appear to be driven solely by the former, suggesting that the latter also contribute to the prediction of regional maps (Fig 1C).

Across Calculation (*mean* r_{short} = 0.950 [.038], *mean* r_{long} = 0.940 [.036]), Checkerboard (*mean* r_{short} = 0.960 [.021], *mean* r_{long} = 0.950 [.021]), Sentence Listening (*mean* r_{short} = 0.958 [.031], *mean* r_{long} = 0.947 [.029]), and Sentence Reading (*mean* r_{short} = 0.960 [.026], *mean* r_{long} = 0.946 [.029]), predictive accuracy was significantly higher for short-range than long-range connections ($q < 0.05$). Interestingly, the opposite pattern emerged for the Left (*mean* r_{short} = 0.928 [.038], *mean* r_{long} = 0.932 [.035]) and Right (*mean* r_{short} = 0.931 [.034], *mean* r_{long} = 0.936 [.033]) Button Press conditions, where long-range connections exhibited significantly greater predictive accuracy than short-range connections (Supplementary Table 4)

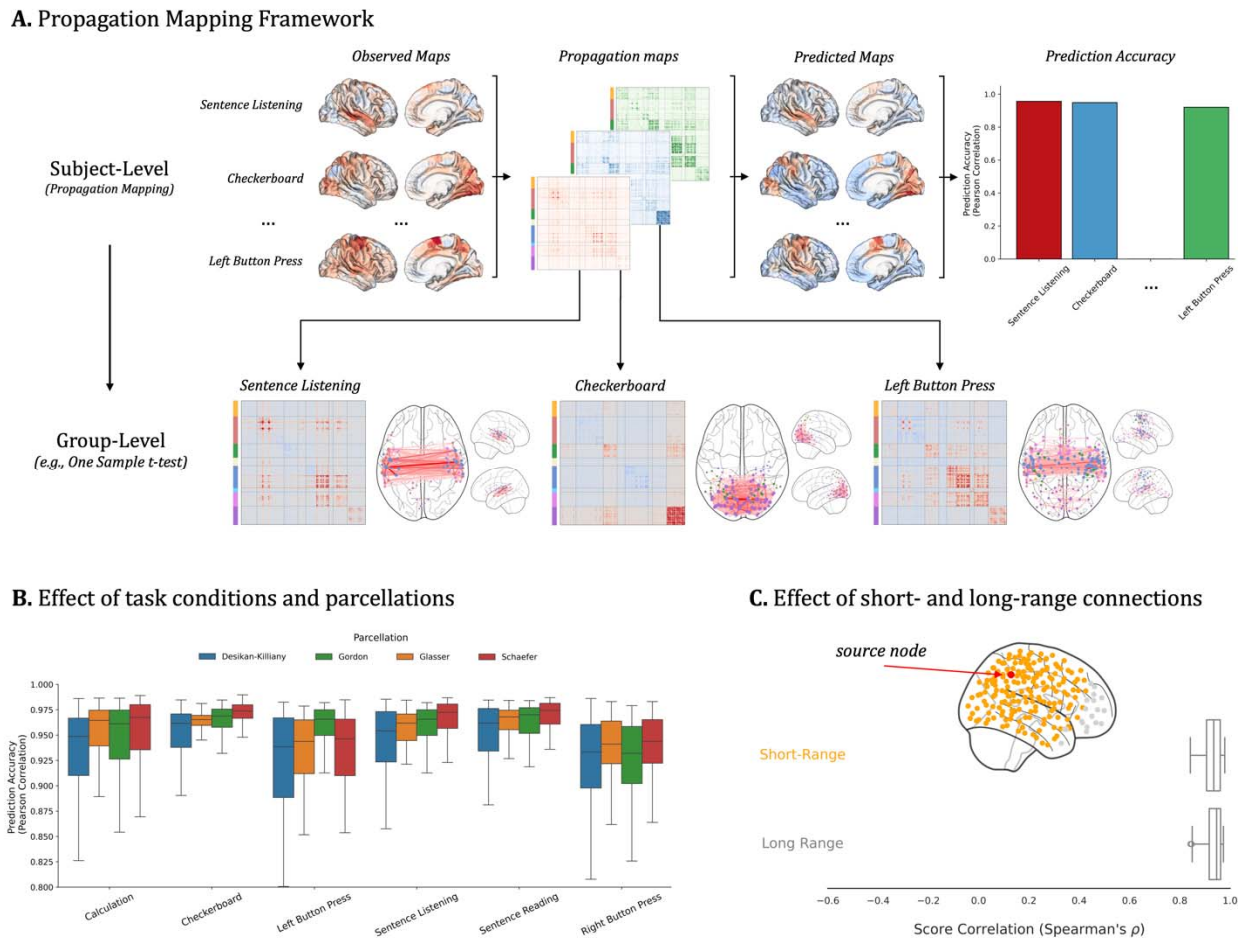

Fig 1. Validity of Propagation Mapping using task-based imaging data. A. Following the method described in the current study, subject-level predictions (n = 94) were made across six contrasts (checkerboard; calculation [auditory & visual]; sentence reading; sentence listening; left and right button press [auditory & visual]) derived from a localizer task [46] as well as four different parcellation atlases [35,40-42]. Prediction accuracies were recorded across subjects, task contrasts, and parcellation atlases. **B.** Bar graphs show the subject-level prediction accuracy across parcellation atlases and task contrasts. Prediction accuracies were near-perfect across task contrasts using Schaefer's parcellation, whereas the Desikan-Killiany anatomical parcellation showed overall lower prediction accuracy compared to the other parcellations, though results were broadly comparable (median $r > 0.90$). **C.** To test whether predictive performance was driven by short-range connections (and potentially spatial autocorrelation), distance-based cross-validation was conducted. The training set consisted of the 75% of regions nearest to each source node in surface space, and the test set consisted of the 25% of regions farthest from the source node. Predictive accuracy of propagation mapping was aggregated across each source node iterations for the training (short-range connections) and test (long-range connections) sets for each subject. Findings indicate that both short-range and long-range connections contribute equally to the predictive accuracy of propagation mapping.

Results: Study 2

Group-level Predictive Accuracy

Using an independent sample (n = 228), we tested the replicability of propagation mapping's predictive accuracy with low-frequency oscillations of the resting-state BOLD signal, namely ALFF and fALFF maps. The predicted maps, derived from group-level propagation maps, showed comparable predictive accuracy to that observed in Study 1 for both ALFF (r = 0.97) and fALFF (r = 0.96) (Fig. 2A). These findings suggest that propagation mapping yields stable predictive accuracy while retaining group-level information, providing a useful measure for comparing group differences.

Functional Fingerprint

Each subject's ALFF- and fALFF-based propagation maps were then used to examine whether the current method preserves individual uniqueness in brain functioning, as demonstrated by greater self-identifiability relative to other-identifiability (Fig. 2B). Average Identifiability across subjects was 0.939 (SD = 0.133), suggesting that indeed propagation mapping preserves individual neural fingerprint. Subsequent analyses showed, similar to what others observed using traditional FC, that identification accuracy was generally higher for between-network connectivity compared to within-network connectivity. Indeed, near perfect identification accuracy was found for between-network propagation in the Visual (98.5%, SD=9.7%), Dorsal Attention (97.5%, SD=12.2%), Default Mode (96.5%, SD=13.5%), and Somatomotor (96.2%, SD=14.9%) networks

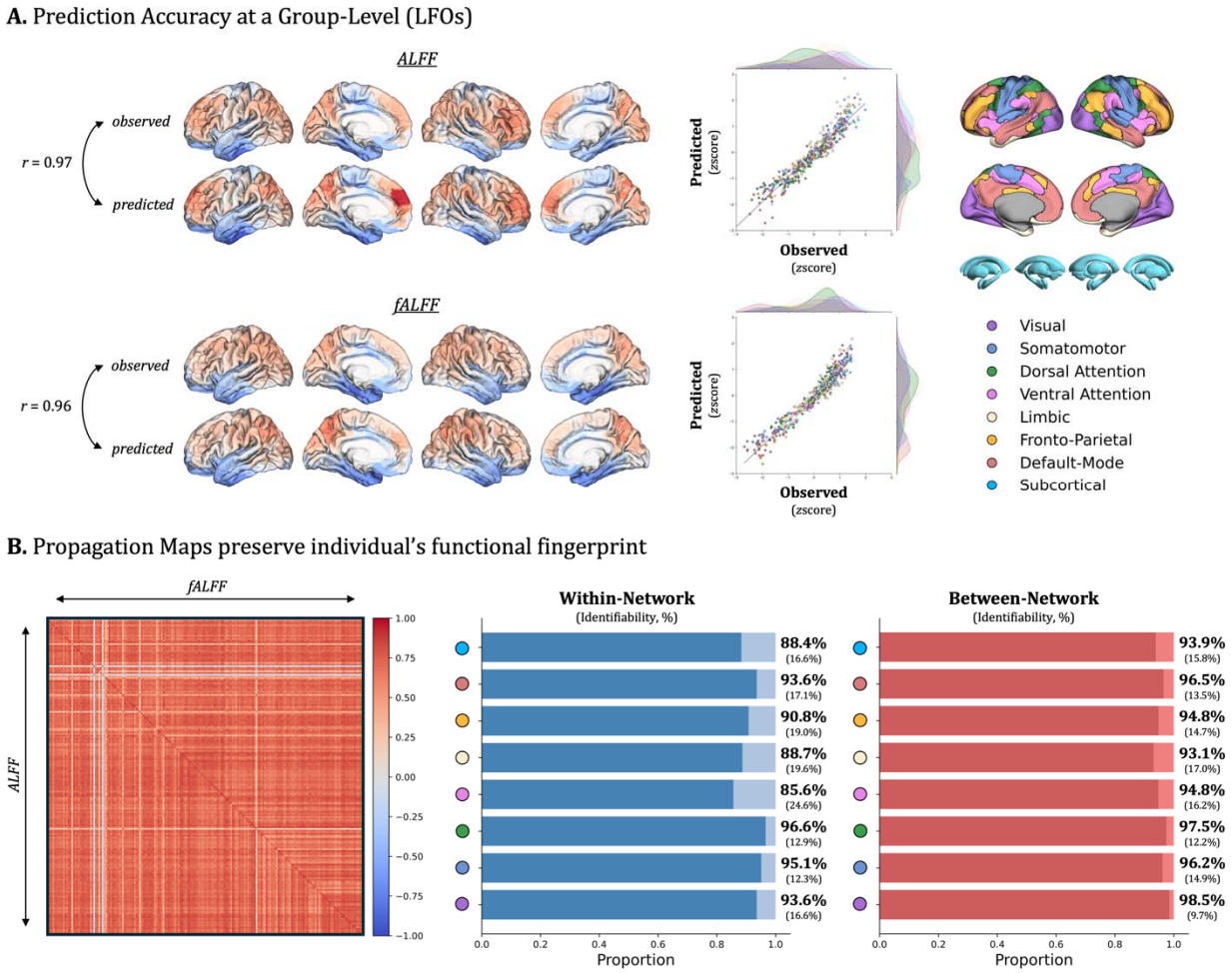

Fig 2. Validity of Propagation Mapping using resting-state neuroimaging data. A. Propagation mapping was applied across subject's resting-state spontaneous brain activity measures (amplitude low frequency fluctuations [ALFF] and its fractional measure relative to the entire frequency range [fALFF]). One sample t-test was conducted on the subject's propagation maps to derive a group-level connectome for each of the spontaneous brain activity measures. Rows of these unthresholded connectomes were summed to get a predicted regional map which was compared against the original group-level regional map. Results showed that propagation mapping captures group-level information at a circuit-level, as demonstrated by very high prediction accuracy at a group-level. **B.** Functional fingerprint analyses were carried out to assess whether relying on group-level estimates from a large sample of healthy subjects may reduce inter-individual differences in brain maps. Findings shows that propagation mapping preserves individual's unique spatial organization. LFOs = Low Frequency Oscillations.

Discussion

The goal of the current study was to introduce and validate *propagation mapping*, a novel framework that reconstructs the connectome underlying the spatial organization of human brain maps. Similar to Cole and colleagues [23] 's seminal work, I show that resting-state FC can indeed predict the spatial organization of task-evoked activity. More importantly, near-perfect prediction of subject-level task-evoked activity map can be achieved by also taking into account SC patterns generated from a large sample of healthy subjects. High predictive accuracy was consistent across multiple task contrasts, parcellation atlases, and across distance of connections. I further demonstrate that propagation mapping preserves each individual's functional fingerprint, highlighting its suitability for studying inter-individual differences in brain–behavior relationships. Overall, this study offers a comprehensive biological insight into the spatial organization of brain mapping. Indeed, these results suggest that, despite widespread variability in regional brain maps, the underlying functional architecture remains stable and can be inferred from integrated network properties. Propagation mapping is a reliable and easy to use tool to capture the neural architecture underlying human brain maps, opening new possibilities for personalized neuroscience and precision psychiatry.

Beyond methodological advances, propagation mapping offers conceptual and biological insights into brain organization. Findings of the current study underscore that regional activity and connectivity are not mutually exclusive measures but fundamentally interdependent. Taken separately, both methods appeared to miss a critical piece of the biological puzzle. Propagation mapping aims to overcome these issues. Indeed, it challenges the traditional assumption that brain regions operate as isolated units, but also highlight the importance of considering signal amplitude in connectivity-based approaches. Consequently, propagation mapping explicitly

adopts an integrative view to reconstruct the neural circuitry that gives rise to the regional variation of a brain map. Previously, Cole and colleagues [23] showed that multivariate regression to model FC led to greater predictive accuracy relative to bivariate correlation. Here, I demonstrate that correlation does capture near perfect prediction accuracy at a subject-level. Indeed, simpler bivariate models can still capture the core architecture of brain's spatial patterns, compared to more sophisticated models aiming at isolating unique influences between regions as a proxy measure of effective connectivity [59]. Relative to prior work [23], it can be inferred that better performance was responsible due to the 1) stability of group-level connectivity estimates, which were derived from a large sample of healthy subjects, and the 2) additional biological constraint of structural covariance on functional connectivity. A series of biological models were tested to explore the performance of propagation mapping. Analyses revealed that predictive accuracy was lowest when using FC alone, but improved significantly when incorporating SC as a biological constraint. Moreover, positive edges alone contributed substantially to predictive accuracy compared to the full connectivity range, indicating that negative edges (or anti-correlations) play little role in reconstructing the spatial arrangement of regional maps. This aligns with prior work showing greater reliability of positive compared to negative correlations [60] and supports the idea that positive connections form the core architecture underlying brain spatial organization [25-27].

Throughout this study, I showed that it is possible to accurately map the neural circuitry underlying a given brain map at both a subject- and group-level. More importantly, the accuracy is stable and replicable across different tasks, different participants, different parcellations, different levels of analysis (i.e., subject- & group-level). Furthermore, it preserves functional fingerprint identifiability, rendering propagation mapping as a reliable tool to study inter-

individual differences in propagation maps. Overall, propagation mapping offers a novel framework for precision brain mapping and expands the potential avenues for neuroimaging research. For example, it is plausible that propagation mapping on resting-state BOLD activity, acquired for an adequate scan length (20 min, [61]), would capture a more stable organization than traditional connectivity-based approaches, leading to better test-retest reliability. It could be assumed that regional changes are more prone to variability than the sum of the connectivity to hundreds of parcels, especially if the core architecture is stable and estimated across thousands of subjects. Researchers are strongly encouraged to examine the test-retest reliability of this method, in comparison to traditional approach that relies on univariate assumption of the brain. Other potential benefits of using propagation mapping include the generation of novel research using static images. Indeed, connectivity-based inferences remain challenging for many modalities (e.g., Positron emission tomography, structural imaging, imaging transcriptomics), although some group-level approaches based on inter-individual covariance have been proposed [30,62]. Other advantages of propagation mapping include the calculation of residuals, where deviations of a region from what is typically expected based on connectomes can be interpreted as atypical connectivity. These measures can be further used to explore demographic or clinical correlates. Additionally, computational lesioning can be applied to quantify the importance of individual nodes. For example, identifying a region whose removal strongly disrupts a subject's brain map can be used to explore various scientific questions.

Propagation mapping provides a direct and reliable alternative to characterize the underlying architecture of such maps. I also encourage researchers to explore the usefulness of this method with different type of brain maps (e.g., BOLD, positron emission tomography, structural imaging, imaging transcriptomics) and different level of analyses (e.g., at a subject-,

group-, and even at a meta-analytic level). Overall, this method attempts to reconcile localizationist and connectionist perspectives on the conceptualization of the brain, with the aim of generating new discoveries in neuroscience and psychiatric imaging.

Although the current study highlights many advantages of propagation mapping, several limitations should be acknowledged. First, propagation mapping does not achieve perfect prediction accuracy at the subject level. Therefore, researchers should consider variability in prediction accuracy across individuals as a potential confounder. Second, the current approach assumes linearity in predicting brain maps, which may fail to capture potential nonlinear relationships between brain regions. Third, the method relies on a bivariate approach, meaning that the directionality of signal propagation cannot be determined.

Conclusion

The current study introduced and validated propagation mapping as a reliable and versatile method for reconstructing the architecture underlying brain maps. By integrating group-level FC and SC, propagation mapping achieved near-perfect prediction of subject-level task-evoked and spontaneous brain activity. Its performance was stable across task conditions, parcellation atlases, levels of analysis (subject- and group-level), and both short- and long-range connectivity. Importantly, propagation mapping preserved the uniqueness of each individual's brain activity, highlighting its utility in the study of brain–behavior relationships. Overall, propagation mapping provides the necessary tools to advance precision brain mapping and to open new avenues for personalized neuroscience and psychiatric research.

Method: Propagation Mapping

Normative Sample

One general hypothesis of the current study was that regional maps may operate on a general and stable functional architecture. Therefore, prediction of brain maps is assumed to benefit from using group-level connectomes derived from healthy subjects, as they show more stable and reliable FC estimates. Therefore, the prediction was conducted by utilizing group-level FC and SC estimates generated from 1000 healthy subjects (ages 18–35 years old, 50□% females) of the Brain Genomics Superstruct Project [33,34]. Data acquisition and Information about preprocessing steps of functional neuroimaging data is available elsewhere [34] and in Supplementary Material.

For each participant, the denoised brain activity signal was extracted from 421 regions, including 400 cortical [35], 14 subcortical [36], and 7 cerebellar [37] regions for each participant. Correlations were then calculated between the activity of each region and all other regions, producing a connectivity matrix for each individual. These correlation values were converted into standardized scores (z-scores) to allow comparison and subsequently averaged across all 1,000 participants, to generate a group-level FC matrix.

As detailed elsewhere [38], structural data was preprocessed using the Computational Anatomy Toolbox (CAT12) within the Statistical Parametric Mapping 12 (SPM12) software [39]. As recommended [39], weighted overall quality rating (IQR) and quartic mean z-scores were used to measure data homogeneity before and after pre-processing. Data with z-scores higher than 2 will be visually inspected to detect potential artefacts. For each subject, mean volume of each of the parcels from the 421 regions (see above) were extracted as well as total intracranial volume (TIV). Group-level structural covariance was estimated by conducting partial correlation

between the mean volume of each of the 421 regions, while adjusting for TIV. Coefficients were converted to normally distributed z-scores using Fisher's r-to-z transformation.

Because the study aims to examine the stability of propagation mapping's predictive accuracy across different parcellation atlases, FC and SC matrices were generated for multiple widely used atlases: an anatomical atlas (Desikan-Kiliany Atlas, 68 cortical regions, [40]), resting-state (Gordon Atlas, 333 parcels, [41]) and multi-modal atlas (Glasser HCP-MMP1, 360 parcels, [42]). Each parcellation was supplemented with the same 14 subcortical and 7 cerebellar regions as described above to ensure comparability.

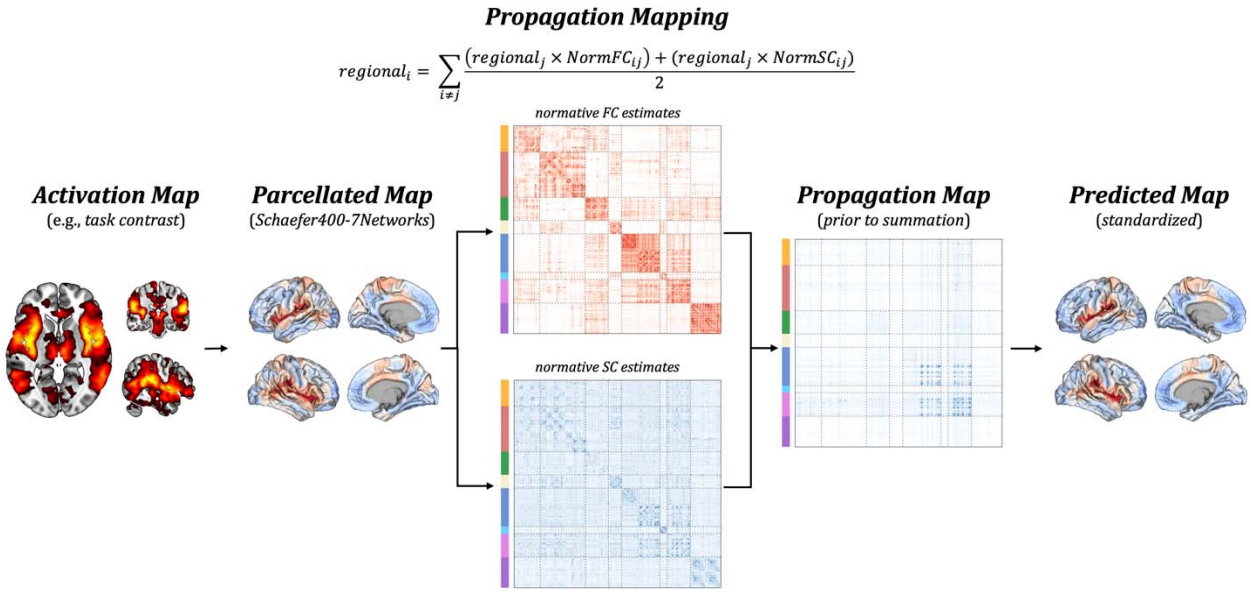

Fig 3. Development of Propagation Mapping. This method aims to reconstructs the neural circuitry underlying regional brain maps. A voxelwise brain map is first parcellated using the commonly used Schaefer-400 7 networks with additional 14 subcortical and 7 cerebellar regions. Each row of the group-level FC and SC matrices (n = 1000, GSP1000) are then multiplied by resulting parcellated feature vector, with the diagonal set to zero to prevent data leakage during prediction. Averaging these weighted matrices produces a propagation map that, when summed, reconstructs the spatial organization of the original brain map.

Statistical Modeling

For each participant, *propagation mapping* was conducted to reconstruct the neural circuitry characterizing their own regional spatial pattern. As shown in Fig 3, raw statistical images are first parcellated using a common parcellation atlas. Building on previous work (Cole et al., 2016), each participant's regional map is then predicted through a weighted sum formula using stable FC and SC estimates (see above). The inclusion of SC estimates into the prediction model is justified given its critical role in shaping brain function [43-45]:

For each target region i, the predicted regional measure ($regional_i$), is calculated as the sum over all other regions $i \neq j$ of the average contribution from FC and SC. Specifically, for each region j, the regional measure at that region ($regional_j$) is multiplied by its FC with region i ($NormFC_{ij}$) and by its SC with region i ($NormSC_{ij}$). These two products are then averaged, and the resulting value is then summed across all regions $i \neq j$ to generate the predicted value for region i. For each participant, prediction accuracy was quantified as the Pearson correlation between the observed (raw parcellated image) and predicted map. The core idea behind propagation mapping lies in that if spatial organization of brain maps can be accurately predicted by a weighted sum, this indicate that the weighted connectome—prior to summation—faithfully captures the connectivity patterns underlying a given spatial pattern. This reconstructed connectome, referred to as a *propagation map*, may then be used to generate new hypotheses through graph metrics and connectome-based predictive modeling.

Method: Study 1

Study sample and Design

A first study was conducted to test the reliability of propagation mapping across different subjects, task-evoked contrasts, parcellation atlases, and across short-range and long-range connections. Data used for this current study was obtained from the Brainomics/Localizer dataset [46,47], A subset of 94 participants was made openly available (see https://osf.io/vhtf6), which include 49 women and 45 men, with a mean age of 24.7 years old (18-49 years old). The Localizer study received ethical approval from their Local ethics committee, and all subjects

provided informed consent [46,47]. Data acquisition and preprocessing can be found elsewhere [46,47] and in Supplementary Material.

The Localizer task included ten trial types that were presented to participants. From these trial types, 6 task contrasts were selected in the current study given their neurobiological differences, to examine the predictive accuracy of propagation mapping: 1) Checkerboard (i.e., passive viewing of flashing checkerboards), 2) Sentence Reading (i.e., silently reading short visual sentences), 3) Sentence Listening (i.e., listening to short sentences). 4) Calculation (i.e., solving silently visual/auditory subtraction problems, 5) Left Button Press (i.e., pressing the left button with the left thumb according to the auditory/visual instruction), and 6) Right Button Press (i.e., pressing the right button with the right thumb according to the auditory/visual instruction).

Statistical Analyses

Predictive Accuracy: Biological Models

To identify the most optimal biological model for propagation mapping, I tested predictive accuracy across seven different approaches: (a) using the full FC only; (b) using only positive edges of the FC; (c) using the full SC matrix only; (d) using only positive edges of the SC; (e) combining the full FC and SC matrices with equal weighting; (f) combining the positive edges of the FC and SC matrices with equal weighting; and (g) a map-specific unequal weighting between FC and SC, defined as $([1 - \alpha] \times FC) + (\alpha \times SC)$ with the best predictive accuracy was selected by testing 1000 possible values of α ranging from 0 to 1, accounting for potential variations in the structural constraint on FC.

Predictive Accuracy: Task Contrasts & Parcellations

Prediction accuracy of propagation mapping was tested across multiple parcellations to rule out the possibility that the findings were driven by a specific parcellation and to test that the method generalizes well across different parcellation atlases. To do so, 3 widely used cortical parcellations were included in the analyses including an anatomical (68 cortical regions, [40]), resting-state (333 parcels, [41]) and multi-modal atlas (360 parcels, [42]). These were supplemented by additional 14 subcortical regions [36] and 7-cerebellar [37] regions to allow comparability. Non-parametric one-way repeated measures analysis of variance by rank, known as Friedman test, was conducted to examine the differences in predictive accuracy between the different parcellations atlases. Pairwise differences were further explored with Wilcoxon signed–rank tests. Significance was set at $q<0.05$ after correction for multiple comparisons [48].

Predictive Accuracy: Short-range vs. Long-range Connections

To better describe the significance of propagation mapping, further analyses were carried out to explore whether prediction accuracy might have been driven by short-range connections. More importantly, because spatial autocorrelation might inflate the estimated association between brain maps [49,50], and therefore the prediction accuracy in the current study, a distance-dependent cross-validation was performed [51,52]. For each cortical region of the Schaefer-400 atlas (source node), the 75% nearest regions to each seed region in surface space were selected as the training set (short-range connections), leaving the remaining 25% of regions farthest from the seed region for the test set (long-range connections). Predictive accuracy of propagation mapping was aggregated across each seed region for the training (short-range connections) and test (long-range connections) sets for each subject. Pairwise differences between subject's short-range and

long-range prediction accuracy were calculated with Wilcoxon signed–rank tests ($q<0.05$ after correction for multiple comparisons, [48].

Method: Study 2

Study sample and Design

A second study was conducted to examine the replicability of predictive accuracy of propagation mapping using resting-state spontaneous brain activity, as well as to validate whether propagation mapping preserves subject's unique brain organization. To do so, neuroimaging data from 227 healthy individuals (82 females, age range 20-77 years old) were derived from the publicly available Mind-Brain-Body dataset from the Max Planck Institute for Human and Cognitive and Brain Sciences [53]. Participants resting-state MRI session for a duration of 15 min 30. Data acquisition and preprocessing can be found elsewhere [53] and in Supplementary Material.

Statistical Analyses

<u>Predictive Accuracy: Spontaneous Brain Activity</u>

Predictive accuracy of propagation mapping was tested using low frequency oscillations of BOLD signal at rest. This was captured by amplitude of low frequency fluctuations (ALFF) which assess the strength of spontaneous neural activity within the low frequency band [54]. ALFF is calculated as the root mean square of BOLD signal at each individual voxel after band-pass filtering [55]. Although ALFF shows moderate to high test-retest reliability [14], it is also sensitive to physiological noise. Therefore, fractional ALFF (fALFF) was also computed by taking the power of low frequency range divided by the total power of entire frequency range [56].

First, group-level ALFF and fALFF regional maps were generated using one-sample permutation tests across all 189 subjects who passed quality assurance. These group-level maps were then parcellated with 421 regions (see above). Second, a propagation map was generated for each subject, resulting in 189 ALFF-based and 189 fALFF-based propagation maps. Group-level propagation maps were then computed via one-sample permutation tests across subjects' ALFF- and fALFF-based maps, using Network-Based Statistics toolbox [57]. Because the study's goal was to assess the predictive accuracy of propagation mapping rather than the statistical significance of individual edges, the rows of the group-level unthresholded propagation maps were summed to generate a predicted map. Finally, predictive accuracy was quantified as the Pearson correlation between the observed group-level ALFF/fALFF and the predicted map.

Functional Fingerprint

Growing evidence suggests that individuals exhibit unique brain activity patterns, often referred to as neural fingerprints [31,32]. Since propagation mapping relies on group-level FC and SC derived from an independent sample (GSP1000), the method may obscure subject's uniqueness and therefore limit its utility for studying inter-individual differences. To assess this, I investigated whether the reconstructed propagation maps preserve an individual's functional fingerprint. Specifically, for each subject (*s*), propagation maps (*PM*) were generated from the two measures of spontaneous brain activity, namely ALFF & fALFF. For each subject, the upper diagonal of the propagation map was stacked into a vector (88,410, edges). A within-subject similarity (*ISelf*) was first defined as the Pearson correlation between subject *s*'s ALFF-based and fALFF-based propagation maps:

$$ISelf(s) = corr(PM_{ALFF}(s), PM_{fALFF}(s))$$

A between-subject similarity (*IOther*) was then defined as the average correlation between subject *s*'s propagation maps (PM_{ALFF} & PM_{fALFF}) with those of all other subjects ($i \neq s$), where *N* is the total number of subjects[58]:

$$IOther(s) = \frac{\sum_{i \neq s}(corr(PM_{ALFF}(s),\ PM_{fALFF}(i)) + (corr(PM_{fALFF}(s), PM_{ALFF}(i)))}{2N - 2}$$

Finally, identification accuracy was calculated as the percentage of cases in which the within-subject similarity (*ISelf*, diagonal elements of the matrix) exceeded the between-subject similarity (*IOthers*, off-diagonal elements of the matrix). To assess the contribution of intrinsic connectivity networks to the identifiability, identification accuracy was computed separately for within- and between-network connections across each of the 7 Schaefer's canonical networks.

Acknowledgements

I would like to thank Dr. Stéphane De Brito for his incommensurable support over the past years, which made this possible. This study did not receive any specific funding.

Authors Contributions

J.R.D. designed the study, performed all analyses, and wrote and approved the final version of the manuscript.

Competing Interests

The author declares no potential conflict of interest.

Data Availability

The Brain Genomics Superstruct Project (https://dataverse.harvard.edu/dataverse/GSP), Mind-Brain-Body dataset from the Max Planck Institute for Human and Cognitive and Brain Sciences (https://fcon_1000.projects.nitrc.org/indi/retro/MPI_LEMON.html), and Brainomics/Localizer dataset (https://osf.io/vhtf6/) are openly available.

Code Availability

Propagation Mapping Toolbox is a user friendly toolbox that was made freely available on Streamlit Cloud (https://propagation-mapping.streamlit.app/) or locally (https://github.com/JulDugre/Propagation-Mapping).

References

1 Wright, I. C. *et al.* A voxel-based method for the statistical analysis of gray and white matter density applied to schizophrenia. *Neuroimage* **2**, 244-252 (1995). https://doi.org/10.1006/nimg.1995.1032

2 Fox, P. T. *et al.* Mapping human visual cortex with positron emission tomography. *Nature* **323**, 806-809 (1986). https://doi.org/10.1038/323806a0

3 Friston, K. J. *et al.* Spatial registration and normalization of images. *Human Brain Mapping* **3**, 165-189 (1995). https://doi.org/https://doi.org/10.1002/hbm.460030303

4 Friston, K. J., Penny, W. D., Ashburner, J., Kiebel, S. J. & Nichols, T. E. *Statistical parametric mapping : the analysis of functional brain images.* 656 (Academic Press, 2006).

5 Elliott, M. L. *et al.* What Is the Test-Retest Reliability of Common Task-Functional MRI Measures? New Empirical Evidence and a Meta-Analysis. *Psychol Sci* **31**, 792-806 (2020). https://doi.org/10.1177/0956797620916786

6 Guo, Q. *et al.* The reporting of observational clinical functional magnetic resonance imaging studies: a systematic review. *PLoS One* **9**, e94412 (2014). https://doi.org/10.1371/journal.pone.0094412

7 Botvinik-Nezer, R. *et al.* Variability in the analysis of a single neuroimaging dataset by many teams. *Nature* **582**, 84-88 (2020). https://doi.org/10.1038/s41586-020-2314-9

8 Demidenko, M. I., Mumford, J. A. & Poldrack, R. A. Impact of analytic decisions on test-retest reliability of individual and group estimates in functional magnetic resonance imaging: A multiverse analysis using the monetary incentive delay task. *Imaging Neurosci (Camb)* **2** (2024). https://doi.org/10.1162/imag_a_00262

9 Noble, S., Curtiss, J., Pessoa, L. & Scheinost, D. The tip of the iceberg: A call to embrace anti-localizationism in human neuroscience research. *Imaging Neurosci (Camb)* **2** (2024). https://doi.org/10.1162/imag_a_00138

10 Segal, A. *et al.* Embracing variability in the search for biological mechanisms of psychiatric illness. *Trends Cogn Sci* **29**, 85-99 (2025). https://doi.org/10.1016/j.tics.2024.09.010

11 Noble, S., Scheinost, D. & Constable, R. T. A decade of test-retest reliability of functional connectivity: A systematic review and meta-analysis. *Neuroimage* **203**, 116157 (2019). https://doi.org/10.1016/j.neuroimage.2019.116157

12 Birn, R. M. *et al.* The effect of scan length on the reliability of resting-state fMRI connectivity estimates. *Neuroimage* **83**, 550-558 (2013). https://doi.org/10.1016/j.neuroimage.2013.05.099

13 Zuo, X. N. & Xing, X. X. Test-retest reliabilities of resting-state FMRI measurements in human brain functional connectomics: a systems neuroscience perspective. *Neurosci Biobehav Rev* **45**, 100-118 (2014). https://doi.org/10.1016/j.neubiorev.2014.05.009

14 Zuo, X. N. *et al.* The oscillating brain: complex and reliable. *Neuroimage* **49**, 1432-1445 (2010). https://doi.org/10.1016/j.neuroimage.2009.09.037

15 Sbaihat, H. *et al.* Test-retest stability of spontaneous brain activity and functional connectivity in the core resting-state networks assessed with ultrahigh field 7-Tesla resting-state functional magnetic resonance imaging. *Hum Brain Mapp* **43**, 2026-2040 (2022). https://doi.org/10.1002/hbm.25771

16 Biswal, B., Yetkin, F. Z., Haughton, V. M. & Hyde, J. S. Functional connectivity in the motor cortex of resting human brain using echo-planar MRI. *Magn Reson Med* **34**, 537-541 (1995). https://doi.org/10.1002/mrm.1910340409

17 Di, X. *et al.* The influence of the amplitude of low-frequency fluctuations on resting-state functional connectivity. *Front Hum Neurosci* **7**, 118 (2013). https://doi.org/10.3389/fnhum.2013.00118

18 Garrett, D. D., Epp, S. M., Perry, A. & Lindenberger, U. Local temporal variability reflects functional integration in the human brain. *Neuroimage* **183**, 776-787 (2018). https://doi.org/10.1016/j.neuroimage.2018.08.019

19 Liang, X., Zou, Q., He, Y. & Yang, Y. Coupling of functional connectivity and regional cerebral blood flow reveals a physiological basis for network hubs of the human brain. *Proc Natl Acad Sci U S A* **110**, 1929-1934 (2013). https://doi.org/10.1073/pnas.1214900110

20 Sheng, J. *et al.* The coupling of BOLD signal variability and degree centrality underlies cognitive functions and psychiatric diseases. *NeuroImage* **237**, 118187 (2021). https://doi.org/https://doi.org/10.1016/j.neuroimage.2021.118187

21 Castrillon, G. *et al.* An energy costly architecture of neuromodulators for human brain evolution and cognition. *Sci Adv* **9**, eadi7632 (2023). https://doi.org/10.1126/sciadv.adi7632

22 Wu, C. W. *et al.* Mapping functional connectivity based on synchronized CMRO2 fluctuations during the resting state. *Neuroimage* **45**, 694-701 (2009). https://doi.org/10.1016/j.neuroimage.2008.12.066

23 Cole, M. W., Ito, T., Bassett, D. S. & Schultz, D. H. Activity flow over resting-state networks shapes cognitive task activations. *Nat Neurosci* **19**, 1718-1726 (2016). https://doi.org/10.1038/nn.4406

24 Cocuzza, C. V., Sanchez-Romero, R. & Cole, M. W. Protocol for activity flow mapping of neurocognitive computations using the Brain Activity Flow Toolbox. *STAR Protoc* **3**, 101094 (2022). https://doi.org/10.1016/j.xpro.2021.101094

25 Cole, M. W., Bassett, D. S., Power, J. D., Braver, T. S. & Petersen, S. E. Intrinsic and task-evoked network architectures of the human brain. *Neuron* **83**, 238-251 (2014). https://doi.org/10.1016/j.neuron.2014.05.014

26 Gratton, C. *et al.* Functional Brain Networks Are Dominated by Stable Group and Individual Factors, Not Cognitive or Daily Variation. *Neuron* **98**, 439-452.e435 (2018). https://doi.org/10.1016/j.neuron.2018.03.035

27 Smith, S. M. *et al.* Correspondence of the brain's functional architecture during activation and rest. *Proc Natl Acad Sci U S A* **106**, 13040-13045 (2009). https://doi.org/10.1073/pnas.0905267106

28 Shen, X. *et al.* Using connectome-based predictive modeling to predict individual behavior from brain connectivity. *Nat Protoc* **12**, 506-518 (2017). https://doi.org/10.1038/nprot.2016.178

29 Mechelli, A., Friston, K. J., Frackowiak, R. S. & Price, C. J. Structural covariance in the human cortex. *J Neurosci* **25**, 8303-8310 (2005). https://doi.org/10.1523/jneurosci.0357-05.2005

30 Alexander-Bloch, A., Giedd, J. N. & Bullmore, E. Imaging structural co-variance between human brain regions. *Nat Rev Neurosci* **14**, 322-336 (2013). https://doi.org/10.1038/nrn3465

31 Amico, E. & Goñi, J. The quest for identifiability in human functional connectomes. *Scientific Reports* **8**, 8254 (2018). https://doi.org/10.1038/s41598-018-25089-1

32 Finn, E. S. *et al.* Functional connectome fingerprinting: identifying individuals using patterns of brain connectivity. *Nature Neuroscience* **18**, 1664-1671 (2015). https://doi.org/10.1038/nn.4135

33 Holmes, A. J. *et al.* Brain Genomics Superstruct Project initial data release with structural, functional, and behavioral measures. *Sci Data* **2**, 150031 (2015). https://doi.org/10.1038/sdata.2015.31

34 Yeo, B. T. *et al.* The organization of the human cerebral cortex estimated by intrinsic functional connectivity. *J Neurophysiol* **106**, 1125-1165 (2011). https://doi.org/10.1152/jn.00338.2011

35 Schaefer, A. *et al.* Local-Global Parcellation of the Human Cerebral Cortex from Intrinsic Functional Connectivity MRI. *Cereb Cortex* **28**, 3095-3114 (2018). https://doi.org/10.1093/cercor/bhx179

36 Fischl, B. *et al.* Whole brain segmentation: automated labeling of neuroanatomical structures in the human brain. *Neuron* **33**, 341-355 (2002). https://doi.org/10.1016/s0896-6273(02)00569-x

37 Buckner, R. L., Krienen, F. M., Castellanos, A., Diaz, J. C. & Yeo, B. T. The organization of the human cerebellum estimated by intrinsic functional connectivity. *J Neurophysiol* **106**, 2322-2345 (2011). https://doi.org/10.1152/jn.00339.2011

38 Dugré, J. R. *et al.* Mapping the Structural Brain Network of Psychopathy: Convergent Evidence from Humans and Chimpanzees. *BioRxiv* (2025).

39 Gaser, C. *et al.* CAT: a computational anatomy toolbox for the analysis of structural MRI data. *Gigascience* **13** (2024). https://doi.org/10.1093/gigascience/giae049

40 Desikan, R. S. *et al.* An automated labeling system for subdividing the human cerebral cortex on MRI scans into gyral based regions of interest. *Neuroimage* **31**, 968-980 (2006). https://doi.org/10.1016/j.neuroimage.2006.01.021

41 Gordon, E. M. *et al.* Generation and Evaluation of a Cortical Area Parcellation from Resting-State Correlations. *Cereb Cortex* **26**, 288-303 (2016). https://doi.org/10.1093/cercor/bhu239

42 Glasser, M. F. *et al.* A multi-modal parcellation of human cerebral cortex. *Nature* **536**, 171-178 (2016). https://doi.org/10.1038/nature18933

43 Honey, C. J. *et al.* Predicting human resting-state functional connectivity from structural connectivity. *Proc Natl Acad Sci U S A* **106**, 2035-2040 (2009). https://doi.org/10.1073/pnas.0811168106

44 Pang, J. C. *et al.* Geometric constraints on human brain function. *Nature* **618**, 566-574 (2023). https://doi.org/10.1038/s41586-023-06098-1

45 Qing, Z. & Gong, G. Size matters to function: Brain volume correlates with intrinsic brain activity across healthy individuals. *Neuroimage* **139**, 271-278 (2016). https://doi.org/10.1016/j.neuroimage.2016.06.046

46 Papadopoulos Orfanos, D. *et al.* The Brainomics/Localizer database. *Neuroimage* **144**, 309-314 (2017). https://doi.org/10.1016/j.neuroimage.2015.09.052

47 Pinel, P. *et al.* Fast reproducible identification and large-scale databasing of individual functional cognitive networks. *BMC Neurosci* **8**, 91 (2007). https://doi.org/10.1186/1471-2202-8-91

48 Benjamini, Y. & Hochberg, Y. Controlling the False Discovery Rate: A Practical and Powerful Approach to Multiple Testing. **57**, 289-300 (1995). https://doi.org/https://doi.org/10.1111/j.2517-6161.1995.tb02031.x

49 Alexander-Bloch, A. F. *et al.* On testing for spatial correspondence between maps of human brain structure and function. *Neuroimage* **178**, 540-551 (2018). https://doi.org/10.1016/j.neuroimage.2018.05.070

50 Markello, R. D. & Misic, B. Comparing spatial null models for brain maps. *NeuroImage* **236**, 118052 (2021). https://doi.org/https://doi.org/10.1016/j.neuroimage.2021.118052

51 Hansen, J. Y. *et al.* Mapping gene transcription and neurocognition across human neocortex. *Nature Human Behaviour* **5**, 1240-1250 (2021). https://doi.org/10.1038/s41562-021-01082-z

52 Hansen, J. Y. *et al.* Mapping neurotransmitter systems to the structural and functional organization of the human neocortex. *Nat Neurosci* **25**, 1569-1581 (2022). https://doi.org/10.1038/s41593-022-01186-3

53 Babayan, A. *et al.* A mind-brain-body dataset of MRI, EEG, cognition, emotion, and peripheral physiology in young and old adults. *Sci Data* **6**, 180308 (2019). https://doi.org/10.1038/sdata.2018.308

54 Zang, Y. F. *et al.* Altered baseline brain activity in children with ADHD revealed by resting-state functional MRI. *Brain Dev* **29**, 83-91 (2007). https://doi.org/10.1016/j.braindev.2006.07.002

55 Yang, H. *et al.* Amplitude of low frequency fluctuation within visual areas revealed by resting-state functional MRI. *Neuroimage* **36**, 144-152 (2007). https://doi.org/10.1016/j.neuroimage.2007.01.054

56 Zou, Q. H. *et al.* An improved approach to detection of amplitude of low-frequency fluctuation (ALFF) for resting-state fMRI: fractional ALFF. *J Neurosci Methods* **172**, 137-141 (2008). https://doi.org/10.1016/j.jneumeth.2008.04.012

57 Zalesky, A., Fornito, A. & Bullmore, E. T. Network-based statistic: Identifying differences in brain networks. *NeuroImage* **53**, 1197-1207 (2010). https://doi.org/https://doi.org/10.1016/j.neuroimage.2010.06.041

58 Stampacchia, S. *et al.* Fingerprints of brain disease: connectome identifiability in Alzheimer's disease. *Commun Biol* **7**, 1169 (2024). https://doi.org/10.1038/s42003-024-06829-8

59 Friston, K. J. Functional and effective connectivity: a review. *Brain Connect* **1**, 13-36 (2011). https://doi.org/10.1089/brain.2011.0008

60 Shehzad, Z. *et al.* The resting brain: unconstrained yet reliable. *Cereb Cortex* **19**, 2209-2229 (2009). https://doi.org/10.1093/cercor/bhn256

61 Ooi, L. Q. R. *et al.* Longer scans boost prediction and cut costs in brain-wide association studies. *Nature* (2025). https://doi.org/10.1038/s41586-025-09250-1

62 Huang, S. *et al.* Learning brain connectivity of Alzheimer's disease by sparse inverse covariance estimation. *Neuroimage* **50**, 935-949 (2010). https://doi.org/10.1016/j.neuroimage.2009.12.120